

Block Sparse Flash Attention

Daniel Ohayon^{*} ¹ Itay Lamprecht ^{1,2} Itay Hubara ¹ Israel Cohen ¹ Daniel Soudry ¹ Noam Elata ¹

Abstract

Modern large language models increasingly require long contexts for reasoning and multi-document tasks, but attention’s quadratic complexity creates a severe computational bottleneck. We present *Block-Sparse FlashAttention* (BSFA), a drop-in replacement that accelerates long-context inference while preserving model quality. Unlike methods that predict importance before computing scores, BSFA computes exact query-key similarities to select the top- k most important value blocks for each query. By comparing per-block maximum scores against calibrated thresholds, we skip approximately 50% of the computation and memory transfers for pruned blocks. Our training-free approach requires only a one-time threshold calibration on a small dataset to learn the per-layer and per-head attention score distributions. We provide a CUDA kernel implementation that can be used as a drop-in replacement for FlashAttention. On Llama-3.1-8B, BSFA achieves up to 1.10 \times speedup on real-world reasoning benchmarks and up to 1.24 \times for needle-in-a-haystack retrieval tasks while maintaining above 99% baseline accuracy, with certain configurations even improving accuracy by focusing on the most relevant content, substantially outperforming existing sparse attention methods. The implementation is available at <https://github.com/Danielohayon/Block-Sparse-Flash-Attention>.

1. Introduction

Large language models have become the backbone of modern AI systems (et al., 2020; 2023a; OpenAI, 2024), enabling state-of-the-art performance in generation (et al., 2023b), reasoning (Wei et al., 2022; Kojima et al., 2022), and retrieval-augmented applications (Lewis et al., 2020; et al., 2022). At

¹Technion – Israel Institute of Technology, Haifa, Israel ²Intel – Habana Labs, Tel Aviv, Israel. Correspondence to: Daniel Ohayon <ohayon.daniel4@gmail.com>.

^{*}Work was primarily done while at Intel - Habana Labs

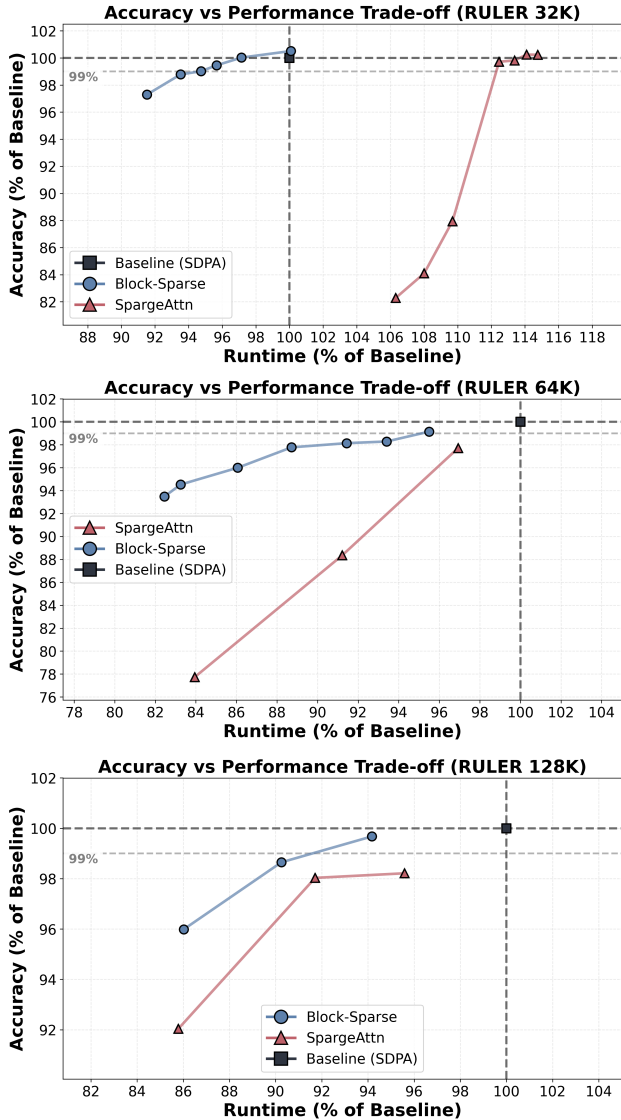


Figure 1. Accuracy-latency trade-offs on RULER for 32K (top), 64K (middle), and 128K (bottom) sequences, with accuracy and speedup measured at the same sequence lengths. BSFA (blue) maintains high accuracy with consistent speedups, outperforming SparseAttention (orange). Each point represents a different sparsity level, see Table 1 for specific configurations.

their core lies scaled dot-product attention, which forms content-dependent weighted averages over contextual representations and thereby gives transformers their remarkable ability to route information flexibly and compose long chains of dependencies (Vaswani et al., 2023). Yet the same mechanism incurs quadratic storage and compute in the sequence length. This tension becomes acute as practitioners push contexts to hundreds of thousands of tokens, where attention operations consume the majority of inference time and can account for over 90% of total FLOPs in long-context scenarios.

A major step forward was to compute exact attention without explicitly forming the full score matrix. FlashAttention reorganizes the computation into tiled streaming updates that keep activations on-chip, reducing the memory footprint from quadratic to linear while preserving numerical exactness (Dao et al., 2022; Dao, 2023). By improving I/O locality and eliminating redundant reads and writes, FlashAttention removes the primary memory bottleneck. However, the arithmetic work of multiplying every query against every key, applying softmax and then applying those weights to values, remains quadratic in sequence length. For long contexts, the computational burden becomes the dominant constraint, as the $O(N^2)$ FLOPs required for attention cannot be reduced without sacrificing exactness.

Empirical evidence demonstrates that attention distributions exhibit natural sparsity, with most tokens concentrating probability mass on small subsets of positions (Section 2.3). This observation has motivated numerous sparse attention methods that reduce computation by avoiding certain query-key interactions (Beltagy et al., 2020; Roy et al., 2020; Kitaev et al., 2020). However, these approaches typically choose to predict importance without observing actual attention scores, potentially missing critical but sparse dependencies. We hypothesize that such predictive early pruning risks accuracy degradation when relevant tokens are scattered unpredictably across long contexts.

We propose Block-Sparse FlashAttention (BSFA), which takes a fundamentally different approach: compute all query-key scores exactly to determine importance, then use these scores to decide which value blocks to process. Unlike methods that must guess importance beforehand, BSFA first computes the exact attention scores between query and key blocks within FlashAttention’s tiled framework. It then skips loading and processing value blocks whose maximum scores fall below calibrated thresholds. This exploits the observation that blocks with uniformly low scores contribute negligibly after softmax normalization. If no query-key pair in a block has high enough similarity, the entire block can be safely skipped without meaningful impact on the output. By preserving exact score computation while selectively skipping value operations, our method achieves significant

speedups without the accuracy risks of early pruning.

Experiments on Llama-3.1-8B demonstrate that BSFA achieves up to $1.10\times$ speedup on real-world reasoning tasks while maintaining 99% of baseline accuracy, with up to $1.24\times$ speedup for needle-in-a-haystack retrieval tasks, substantially outperforming methods that approximate attention scores. We provide a CUDA kernel implementation that extends FlashAttention-2, providing a production-ready solution that can be immediately deployed in real-world applications.

2. Background

2.1. Scaled Dot-Product Attention

Transformers use multi-head scaled dot-product attention to process sequences of tokens (Vaswani et al., 2023). Given a sequence of N tokens with model dimension d_{model} , the input $\mathbf{X} \in \mathbb{R}^{N \times d_{\text{model}}}$ is projected into H attention heads, each with dimension $d = d_{\text{model}}/H$. For each head h :

$$\mathbf{Q}^{(h)} = \mathbf{X}\mathbf{W}_Q^{(h)} \in \mathbb{R}^{N \times d} \quad (\text{queries}) \quad (1)$$

$$\mathbf{K}^{(h)} = \mathbf{X}\mathbf{W}_K^{(h)} \in \mathbb{R}^{N \times d} \quad (\text{keys}) \quad (2)$$

$$\mathbf{V}^{(h)} = \mathbf{X}\mathbf{W}_V^{(h)} \in \mathbb{R}^{N \times d} \quad (\text{values}) \quad (3)$$

where $\mathbf{W}_Q^{(h)}, \mathbf{W}_K^{(h)}, \mathbf{W}_V^{(h)} \in \mathbb{R}^{d_{\text{model}} \times d}$ are learned projection matrices. The attention output for each head is:

$$\begin{aligned} \text{Attention}^{(h)}(\mathbf{Q}^{(h)}, \mathbf{K}^{(h)}, \mathbf{V}^{(h)}) = \\ \underbrace{\text{softmax}\left(\frac{\mathbf{Q}^{(h)}(\mathbf{K}^{(h)})^\top}{\sqrt{d}}\right)}_{\mathbf{P}^{(h)} \in \mathbb{R}^{N \times N}} \mathbf{V}^{(h)} \end{aligned} \quad (4)$$

The outputs from all heads are concatenated (yielding dimension $d_{\text{model}} = H \cdot d$) and then passed through a final linear projection $\mathbf{W}_O \in \mathbb{R}^{d_{\text{model}} \times d_{\text{model}}}$ to mix information across heads. For simplicity of notation, we omit positional encodings (e.g., RoPE) and focus on a single head in subsequent discussions, dropping the superscript (h) .

In standard implementations, the projection matrices $\mathbf{W}_Q, \mathbf{W}_K, \mathbf{W}_V$ are applied to the full d_{model} -dimensional input before splitting into heads. The computational costs are:

- **Linear projections:** $O(Nd_{\text{model}}^2)$ FLOPs total for all $\mathbf{Q}, \mathbf{K}, \mathbf{V}$ projections across all heads.
- **Score computation (QK):** $O(N^2d)$ FLOPs per head, $O(N^2d_{\text{model}})$ total.
- **Softmax normalization:** $O(N^2)$ operations per head, $O(N^2H)$ total.
- **Value aggregation (PV):** $O(N^2d)$ FLOPs per head, $O(N^2d_{\text{model}})$ total.

- **Output projection:** $O(Nd_{\text{model}}^2)$ FLOPs.

For long sequences where $N \gg d_{\text{model}}$, the operations quadratic in N dominate: both the QK score computation and PV aggregation scale as $O(N^2d_{\text{model}})$ while the linear projections scale as $O(Nd_{\text{model}}^2)$. For example, in Llama-3.1-8B with $d_{\text{model}} = 4096$ ($d = 128$, $H = 32$), processing a sequence of $N = 128K$ tokens requires $N^2d_{\text{model}} \approx 6.7 \times 10^{13}$ operations for each of QK and PV, while the linear projections require only $Nd_{\text{model}}^2 \approx 2.1 \times 10^{12}$ operations, yielding a ratio of approximately 32:1. Therefore, optimizing attention for long contexts primarily requires addressing the $O(N^2d)$ complexity of the QK and PV operations.

Beyond computational complexity, memory becomes an equally critical bottleneck. Materializing the full $N \times N$ attention matrix \mathbf{P} requires $O(N^2)$ memory, which becomes prohibitive for long sequences. For instance, storing the attention scores for our 128K example would require over 16 billion elements per head, consuming 32GB in FP16 precision for a single head alone.

2.2. FlashAttention-2: Tiled Computation

FlashAttention-2 (Dao, 2023) computes exact attention without materializing the full $N \times N$ score matrix by using a tiled algorithm with online softmax. The key insight is to partition the computation into blocks and maintain running statistics that allow incremental updates. The algorithm leverages the GPU memory hierarchy, keeping intermediate results in fast on-chip SRAM (Static RAM) while streaming data from slower but larger HBM (High Bandwidth Memory).

The algorithm partitions the query sequence into $M_Q = \lceil N/B_M \rceil$ blocks of size B_M and the key/value sequences into $M_{KV} = \lceil N/B_N \rceil$ blocks of size B_N . Each query block $\mathbf{Q}_i \in \mathbb{R}^{B_M \times d}$ (for $i = 0, \dots, M_Q - 1$) processes all key blocks $\mathbf{K}_j \in \mathbb{R}^{B_N \times d}$ and corresponding value blocks $\mathbf{V}_j \in \mathbb{R}^{B_N \times d}$ (for $j = 0, \dots, M_{KV} - 1$) in sequence.

The key algorithmic innovation is the use of online softmax with incremental updates. Instead of computing and storing the full attention matrix, FlashAttention processes one block at a time and maintains running statistics (maximum values and normalizers) that are updated as each new block is processed. Conceptually, for each query block \mathbf{Q}_i , the algorithm: (1) loads \mathbf{Q}_i from HBM to on-chip memory (shared SRAM and registers) where it remains throughout processing, (2) streams key blocks \mathbf{K}_j from HBM one at a time, (3) computes attention scores $\mathbf{S}_{ij} = \mathbf{Q}_i \mathbf{K}_j^\top / \sqrt{d}$ using tensor cores, with score tiles kept on-chip, (4) updates running statistics (maximum values and normalizers) which are also maintained on-chip, (5) loads the corresponding value block \mathbf{V}_j and accumulates the weighted output in on-chip memory, and (6) rescales the accumulated results

to maintain numerical precision. Throughout the inner loop over key/value blocks, all intermediate results stay on-chip. Only after processing all blocks for a given query block \mathbf{Q}_i is the final output \mathbf{O}_i written back to HBM. The score tiles \mathbf{S}_{ij} are never written to HBM but exist only in on-chip memory during computation. This tiled approach means the full $N \times N$ attention scores matrix is never materialized in memory, fundamentally changing the memory requirements from quadratic to linear. The complete algorithmic details can be found in Dao (2023).

In summary, FlashAttention-2 achieves linear $O(N)$ memory complexity by maintaining only running statistics rather than the full attention matrix, while preserving the $O(N^2d)$ computational complexity of standard attention but with dramatically improved memory access patterns.

The per-tile computational cost reveals why attention remains expensive even with FlashAttention’s memory optimizations. For each tile (i, j) , the algorithm performs two equally expensive matrix multiplications: computing the attention scores $\mathbf{S}_{ij} = \mathbf{Q}_i \mathbf{K}_j^\top$ and applying them to values $\tilde{\mathbf{P}}_{ij} \mathbf{V}_j$, each requiring $2B_M B_N d$ FLOPs. The algorithm must also load both \mathbf{K}_j and \mathbf{V}_j blocks from HBM, with each block containing $B_N d$ elements. Additional overhead from computing exponentials and maintaining running statistics is comparatively minor ($O(B_M B_N)$ operations). Since FlashAttention processes $M_Q \times M_{KV}$ total tiles (approximately half for causal attention), and the QK and PV operations equally dominate the computational cost, each contributes roughly $2N^2 d$ FLOPs to the total complexity.

The key limitation is that while FlashAttention optimizes memory access patterns, it still computes the full dense attention, processing all $O(N^2)$ interactions. This motivates block-sparse approaches that selectively skip blocks with negligible contribution.

2.3. Empirical Sparsity Patterns in Attention

Attention distributions in transformers exhibit predictable sparsity patterns that present opportunities for computational optimization. While attention mechanisms theoretically allow any token to attend to any other token, in practice most attention weights concentrate on a small fraction of positions, with the majority of scores being negligibly small after softmax normalization. Understanding these patterns provides the foundation for designing efficient sparse attention methods.

Origins of sparsity. The sparsity emerges from both theoretical constraints and practical necessities. The phenomenon of *rank collapse* demonstrates that attention matrices degenerate into low-rank forms in deeper layers, fundamentally limiting the model’s capacity to maintain diverse attention patterns across the full context (Dong et al., 2023;

Saada et al., 2025). This mathematical constraint forces models to be selective, concentrating their limited representational capacity on the most informative positions rather than distributing attention uniformly.

Structured patterns. These constraints manifest as structured, predictable patterns across different model architectures and tasks. Models consistently develop *attention sinks* at initial positions, allocating disproportionate probability mass to early tokens to stabilize the softmax computation (Xiao et al., 2024). Beyond these sinks, attention concentrates on sparse “heavy hitter” tokens carrying critical semantic information, while maintaining local attention windows around the current position (Zhang et al., 2023; Zuchet et al., 2025). The remaining positions receive exponentially smaller attention weights, with most query-key interactions contributing negligibly to the final output. This natural sparsity suggests that significant computational savings are possible if one can reliably identify and skip the negligible interactions without compromising model quality (Tang et al., 2024).

3. Related Work

As transformers scale to longer contexts, various approaches have emerged to reduce attention’s quadratic complexity. Since attention consists of three main operations (computing QK scores, applying softmax, and computing PV products), different methods target different subsets of these operations. We categorize existing work by which operations they optimize and when sparsity decisions are made.

Pruning before scoring. Methods that avoid computing \mathbf{QK}^\top for certain pairs can theoretically achieve the greatest speedup by eliminating all three operations (QK computation, softmax, and PV multiplication) for pruned blocks. However, these approaches must predict importance without observing the actual attention scores.

Pattern-based approaches fix sparsity patterns a priori: local windows with global tokens (Beltagy et al., 2020), strided patterns (Child et al., 2019), or block-diagonal structures (Gupta et al., 2021). While computationally efficient, these cannot adapt to content-specific importance patterns.

Content-aware methods attempt to predict importance before scoring. Hashing-based approaches (Kitaev et al., 2020) and clustering (Roy et al., 2020) group similar tokens to restrict attention, but grouping precedes scoring and may miss scattered long-range dependencies. Quest (Tang et al., 2024) uses lightweight query-aware heuristics to prune key-value pairs before forming scores, trading exactness for speed.

The most directly comparable approach is SpargeAttention (Zhang et al., 2025b), which employs a two-stage filter-

ing pipeline to reduce attention computations. In the first stage (global filtering), the method performs selective token compression before the main attention kernel. It calculates cosine similarity within each Q and K block to identify self-similar blocks, which are then compressed via mean-pooling into single representative tokens. Blocks with low internal similarity are flagged as “noisy” and always computed to prevent accuracy loss. A lightweight matrix multiplication on these compressed tokens generates a coarse attention map, from which top- k or cumulative distribution strategies select important block pairs, creating a sparse mask for stage two.

The second stage (local filtering) operates inside the CUDA kernel during the FlashAttention loop. This mechanism is motivated by the online softmax update rule, where the output accumulator is updated recursively: $O_{ij} = \text{diag}(\exp(m_{i,j-1} - m_{ij}))O_{i,j-1} + \tilde{P}_{ij}V_j$. For blocks that passed the global filter, the method compares the local block maximum m_{local} against the running global maximum m_{ij} . When the local maximum is significantly smaller than the running maximum (i.e., $\max(m_{\text{local}} - m_{ij}) < \lambda$), the exponential term drives \tilde{P}_{ij} toward zero. Under these conditions, the contribution of the current block becomes negligible, meaning the output accumulator remains virtually unchanged ($O_{ij} \approx O_{i,j-1}$). Based on this logic, the method skips loading the value block V_j and the subsequent PV computation to save memory bandwidth and compute. This PV-skipping mechanism has a fundamentally different motivation from ours: it targets blocks whose scores become effectively zero after exponential scaling, while our approach directly selects the top- k most important blocks based on their maximum attention scores before softmax normalization.

This approach faces several limitations. First, the global filtering stage must commit to pruning decisions based on approximate, compressed scores, potentially missing sparse but critical interactions. Second, the PV-skipping logic relies on comparison with the running maximum, which varies unpredictably across sequences and positions. Most critically, this creates variable sparsity where different query positions and attention heads may process vastly different numbers of V blocks. Since GPU kernel performance is determined by the slowest thread, positions that retain many blocks become bottlenecks, limiting overall speedup. This explains why SpargeAttention often achieves minimal or even negative speedups (0.86–0.99 \times) in our experiments despite its aggressive optimizations including INT8 quantization.

Gating after scoring. Some methods make sparsity decisions after computing attention scores, but still face limitations. H2O (Zhang et al., 2023) tracks cumulative attention weights during decoding and evicts low-scoring KV cache

entries. However, it faces two key limitations: (1) tokens deemed unimportant and evicted cannot be recovered if they become critical later, and (2) it targets decode-time memory reduction rather than prefill computation.

StreamingLLM (Xiao et al., 2024) retains initial “attention sink” tokens plus a sliding window. While effective for infinite-length streaming, it uses fixed patterns rather than content-based selection and does not address prefill latency.

Learned sparsity. SparseK (Lou et al., 2024) learns which keys to attend to through a trainable scoring network with differentiable top- k selection. While this yields adaptive, content-aware sparsity with provable linear complexity, it requires modifying the model architecture and fine-tuning. In contrast, our method remains training-free: we calibrate thresholds offline on a small dataset without updating any model weights or introducing learnable components.

Approximation methods. Orthogonal to selection-based sparsity, kernel-based (Choromanski et al., 2022) and low-rank (Xiong et al., 2021) methods replace softmax attention with computationally cheaper approximations. While these offer strong asymptotic complexity guarantees, they fundamentally alter the attention mechanism and require architectural changes.

4. Method

We present Block-Sparse FlashAttention (BSFA), a method that accelerates long-context prefill inference by selecting the top- k most important value blocks for each query using calibrated thresholds. Our approach builds on FlashAttention (Dao, 2023), which already optimizes memory access patterns through tiled computation, but still computes the full dense attention. BSFA introduces a simple yet effective modification: after computing exact query-key scores for a block, we check if any score exceeds a calibrated threshold specific to that layer, head, and position. Blocks with maximum scores below the threshold are not selected, allowing us to skip loading and processing their corresponding value blocks entirely.

The key insight driving our design is that attention naturally exhibits block-level sparsity that can be reliably detected through maximum scores. Unlike methods that must predict importance before computing any scores, we compute all $\mathbf{Q}\mathbf{K}^\top$ products exactly. This preserves the fidelity of attention patterns, ensuring we never miss critical dependencies due to approximate importance estimation. While computing all query-key scores may seem conservative, it enables confident pruning decisions: for long-context prefill, the \mathbf{PV} multiplication and value loading that we skip constitute approximately 50% of attention FLOPs and 50% of HBM bandwidth (detailed in Section 4.3). The result is substantial

speedups without the accuracy risks of early pruning.

Our method operates at block granularity for two fundamental reasons. First, modern GPUs achieve peak efficiency when operations align with tensor core boundaries, making block-wise computation natural. Second, and more importantly, working with blocks allows us to make gating decisions efficiently: a single maximum operation per block determines whether thousands of values need to be loaded from HBM and multiplied by the attention scores. Following FlashAttention’s tiling, we partition the projections $\mathbf{Q}, \mathbf{K}, \mathbf{V} \in \mathbb{R}^{N \times d}$ into blocks of size B_M and B_N respectively, where N is sequence length and d is head dimension. At runtime, we select which off-diagonal blocks to process based on their maximum scores, while always retaining diagonal blocks for causal correctness and local coherence. The number of retained blocks k serves as our sparsity parameter, controlling the accuracy-efficiency trade-off.

An additional advantage of our fixed- k design is improved thread execution alignment. Our approach targets k off-diagonal blocks per position, substantially reducing workload variance compared to variable sparsity methods. This contrasts with variable sparsity approaches where different threads may process different numbers of blocks, leading to thread workload imbalance. Since overall kernel performance is determined by the slowest thread, our uniform workload distribution improves GPU utilization.

4.1. Gating Mechanism

Our gating mechanism determines which value blocks to process by examining the maximum attention score within each query-key block pair. For each block pair (i, j) with $j < i$ in the causal setting, we compute the standard scaled dot-product scores (as defined in Section 2):

$$\mathbf{S}_{ij} = \frac{\mathbf{Q}_i \mathbf{K}_j^\top}{\sqrt{d}} \in \mathbb{R}^{B_M \times B_N} \quad (5)$$

and extract the maximum score:

$$s_{\max}^{(i,j)} = \max_{p,q} [\mathbf{S}_{ij}]_{pq} \quad (6)$$

This maximum score serves as our importance metric for block selection. Our goal is to select the top- k most important blocks for each query, where importance is determined by calibrated thresholds specific to each layer, head, and position. Unlike methods such as SpargeAttention that aim to skip blocks whose post-softmax contributions become numerically negligible (effectively zero after exponential scaling), we explicitly target a fixed number of blocks to retain, ensuring consistent computational workload across different inputs.

The key insight is that block maximum scores provide a reliable signal for importance ranking. Through our calibration process (Section 4.2), we learn the score distributions for each specific layer, head, and sequence position, determining what constitutes a “high enough” score for each head’s unique attention pattern. This transforms the abstract notion of importance into practical, head-specific selection criteria that maintain the top- k blocks while discarding the rest.

We gate each block by comparing its maximum score $s_{\max}^{(i,j)}$ against a calibrated threshold $T_{\ell,h,i}^{(k)}$. If $s_{\max}^{(i,j)} < T_{\ell,h,i}^{(k)}$, we skip the block entirely, its values are neither loaded from HBM nor multiplied by the attention scores, and the block is not incorporated into the running statistics. The threshold depends on four parameters: layer index ℓ , attention head h , query-block position i , and the target sparsity level k (number of off-diagonal blocks to retain). This fine-grained parameterization captures the empirical observation that attention patterns vary significantly across layers (models show local attention in lower layers and increased attention to initial tokens in deeper layers), heads (some heads specialize in local vs. global patterns), and positions (Xiao et al., 2024).

The diagonal blocks (i, i) bypass threshold checking entirely and are always processed. This ensures causal correctness in autoregressive models and preserves local dependencies, which typically carry significant importance regardless of the threshold settings.

4.2. Threshold Calibration

A key enabler of our approach is that attention patterns, while varying across layers and positions, remain relatively consistent across different inputs for a given model. Our experiments validate that calibrated thresholds generalize effectively across diverse inputs and sequence lengths, as demonstrated by the calibration stability in Table 1 and the cross-dataset generalization shown in Table 2. This data independence allows us to calibrate thresholds offline on a small dataset and apply them effectively to new inputs at inference time.

We calibrate a tensor of thresholds $\mathbf{T} \in \mathbb{R}^{S \times L \times H \times \lceil N_{\max} / B_M \rceil}$ where S is the number of sparsity levels, L is the number of layers, H is the number of heads, and N_{\max} is the maximum sequence length during calibration. At inference, selecting sparsity level k extracts the slice $\mathbf{T}[k, :, :, :]$, which provides per-layer, per-head, per-position thresholds.

The calibration procedure computes thresholds by analyzing block importance distributions across a small dataset. For each query position, we sort off-diagonal blocks by their maximum scores and select the threshold that retains exactly the top- k blocks. These thresholds are averaged across

calibration samples to obtain robust estimates that generalize well to new inputs.

Storing multiple sparsity levels (S different values of k) enables dynamic adjustment of the latency-accuracy trade-off at deployment time without recalibration. This flexibility proves valuable in practice: different applications may prioritize speed versus accuracy differently, and specific tasks like information retrieval can use much higher sparsity while maintaining accuracy, as shown in our needle-in-a-haystack experiments (Figure 2). The ability to switch seamlessly between sparsity levels based on the current prompt or task requirements provides significant deployment flexibility.

4.3. Complexity Analysis

By skipping blocks with low maximum scores, BSFA eliminates substantial computation and memory traffic. For each skipped block, we avoid:

Compute operations: The dominant saving comes from skipping the **PV** multiplication, which requires $2B_M B_{ND}$ FLOPs per block, the same cost as the **QK** computation. We also skip exponential computations for softmax ($B_M B_N$ operations), running statistics updates ($O(B_M d)$ operations), and normalizer maintenance ($O(B_M B_N)$ operations).

Memory bandwidth: We avoid loading value blocks from HBM, saving B_{ND} elements per skipped block. Since keys and values are the same size, this represents exactly 50% of the key-value memory traffic.

The overhead of computing block maxima and comparing against thresholds is negligible, as these simple operations pale in comparison to the tensor operations we skip.

Practical Considerations. Storage overhead for the threshold tensor is minimal, for a single sparsity level and $N_{\max} = 65,536$, Llama-3.1-8B requires approximately 5.2×10^5 threshold values, negligible compared to the model’s 8B parameters (0.007%). For sequences not aligned with block boundaries, we pad by repeating the last token to avoid introducing artificial scores that would distort the top- k selection. Sequences exceeding N_{\max} reuse thresholds from position N_{\max} , as attention patterns empirically stabilize in later positions. While presented for causal attention, BSFA extends naturally to bidirectional settings.

4.4. Algorithm and Implementation

Algorithm 1 presents our block-sparse FlashAttention for the causal prefill case. The modification to standard FlashAttention is minimal: we add a gating check after computing each score block but before loading values. The integration requires only a conditional branch in the existing kernel: if $s_{\max}^{(i,j)} < T_{\ell,h,i}^{(k)}$ (where the threshold is specific to layer

ℓ , head h , and position i), we skip value loading and all subsequent operations for that block. Skipped blocks do not participate in the running statistics $(m_i, \ell_i, \mathbf{O}_i)$ maintained by the streaming softmax algorithm.

Algorithm 1 Block-Sparse FlashAttention (simplified for single query block i , causal)

```

1: Input: Query block  $\mathbf{Q}_i \in \mathbb{R}^{B_M \times d}$ , Key blocks  $\{\mathbf{K}_j\}$ ,  

   Value blocks  $\{\mathbf{V}_j\}$ , Thresholds  $T_{\ell, h, i}^{(k)}$ 
2: Initialize:  $m_i = -\infty \cdot \mathbf{1}_{B_M}$ ,  $\ell_i = \mathbf{0}_{B_M}$ ,  $\tilde{\mathbf{O}}_i = \mathbf{0}_{B_M \times d}$  {un-scaled accumulator}
3: Load  $\mathbf{Q}_i$  from HBM to SRAM
4: for each key/value block  $j = 0, \dots, i - 1$  do
5:   Load  $\mathbf{K}_j$  from HBM to SRAM
6:   Compute scores:  $\mathbf{S}_{ij} = \mathbf{Q}_i \mathbf{K}_j^\top / \sqrt{d}$  {in SRAM}
7:   Compute block maximum:  $s_{\max}^{(i, j)} = \max(\mathbf{S}_{ij})$ 
8:   if  $s_{\max}^{(i, j)} > T_{\ell, h, i}^{(k)}$  then
9:     Update row-wise max:  $m_i^{\text{new}} = \max(m_i, \text{rowmax}(\mathbf{S}_{ij}))$ 
10:    Compute  $\tilde{\mathbf{P}}_{ij} = \exp(\mathbf{S}_{ij} - m_i^{\text{new}})$  {stable softmax}
11:    Load  $\mathbf{V}_j$  from HBM to SRAM
12:    Rescale accumulator:  $\tilde{\mathbf{O}}_i \leftarrow \tilde{\mathbf{O}}_i \cdot \text{diag}(\exp(m_i - m_i^{\text{new}}))$ 
13:    Update un-scaled output:  $\tilde{\mathbf{O}}_i \leftarrow \tilde{\mathbf{O}}_i + \tilde{\mathbf{P}}_{ij} \mathbf{V}_j$ 
14:    Update normalizer:  $\ell_i \leftarrow \ell_i \cdot \exp(m_i - m_i^{\text{new}}) + \text{rowsum}(\tilde{\mathbf{P}}_{ij})$ 
15:     $m_i \leftarrow m_i^{\text{new}}$ 
16:   end if
17: end for
18: Process diagonal block  $j = i$  with causal mask applied to  $\mathbf{S}_{ii}$  {always process, no gating}
19: Finalize:  $\mathbf{O}_i \leftarrow \tilde{\mathbf{O}}_i \oslash \ell_i$  {final scaling, element-wise division}
20: Store  $L_i = m_i + \log(\ell_i)$  {logsumexp for backward pass}
21: Return:  $\mathbf{O}_i$ 

```

5. Experimental Evaluation

We evaluate Block-Sparse FlashAttention (BSFA) on diverse long-context benchmarks to demonstrate its effectiveness in reducing prefill latency while maintaining model quality. Our experiments span multiple sequence lengths and compare against state-of-the-art baselines under controlled conditions.

5.1. Experimental Setup

Hardware and implementation. All experiments were conducted on NVIDIA A100 80GB GPUs with CUDA 12.1. We implemented BSFA as a custom CUDA

kernel extending FlashAttention 2 (Dao, 2023), with block dimensions $B_M = 128$ and $B_N = 64$ optimized for A100’s tensor cores. The kernel modifications add threshold-based gating logic with minimal overhead. BSFA uses FP16 precision throughout, maintaining numerical fidelity while achieving speedups through selective computation. Our complete implementation is available at <https://github.com/Danielohayon/Block-Sparse-Flash-Attention>, and all reported results are fully reproducible using the provided scripts.

Model and datasets. We evaluate on Llama-3.1-8B-Instruct (et al, 2024), a state-of-the-art language model supporting contexts up to 128K tokens. Evaluation spans over diverse benchmarks. **LongBench** (Bai et al., 2024): Real-world long-document understanding across multiple domains. **RULER** (Hsieh et al., 2024): Synthetic tasks testing precise retrieval and reasoning over long contexts (32K, 64K, 128k tokens)

Crucially, the calibration and evaluation datasets are disjoint across task categories. RULER contains multiple task categories (Retrieval, Multi-hop Tracing, Aggregation, Question Answering, etc.), which we split into two groups. For threshold calibration, we use 16 samples from the first group of categories. For latency (TTFT) measurement, we select 10 samples per sequence length exclusively from the held-out categories not used during calibration, ensuring our speedup measurements reflect generalization to unseen task types. TTFT exhibits low variance across samples of similar length, making 10 samples sufficient for reliable timing. For LongBench, we select the 10 longest samples to stress-test our method on the most demanding sequences. Furthermore, we use these same thresholds calibrated on RULER for our LongBench evaluation (Table 2), demonstrating strong cross-dataset generalization without any dataset-specific tuning. For accuracy evaluation, we test the full RULER and LongBench benchmarks using the lm-evaluation-harness framework (Gao et al., 2024).

Baselines. We compare against three baselines: **Dense FlashAttention 2**: The exact attention baseline using optimized but dense computation. We use FlashAttention 2 as FlashAttention 3 is optimized for Hopper GPUs (H100) and not available for our A100 hardware. **SpgraveAttention** (Zhang et al., 2025b): The concurrent state-of-the-art sparse attention method that combines sparsity with quantization for Q/K blocks. **Sliding Window**: A fixed-pattern baseline that always attends to the previous w tokens for each query position, where w corresponds to the same number of tokens as BSFA’s block budget (e.g., 80 blocks \times $B_N = 64$ tokens/block = 5,120 tokens). This comparison demonstrates that our content-aware sparsity does not simply converge to a trivial local attention pattern.

For SpageAttention, we follow the authors' recommended configuration: cumulative top- τ selection with $\tau \in \{0.3, 0.4, 0.5, 0.6, \dots\}$ and secondary PV filtering threshold of 15. We use their A100-compatible implementation (`spage_attn_meansim_topk_cuda`), with our CUDA version falling within their recommended range for A100 GPUs. Their implementation quantizes Q and K blocks to INT8 while keeping V in FP16. The original paper reports results using FP8 quantization for V blocks on newer GPUs (Zhang et al., 2025a). While SpageAttention combines sparsity with quantization optimizations, our method achieves competitive speedups using only selective computation in FP16, without requiring quantization. This demonstrates that careful sparsity alone, guided by calibrated thresholds, can match or exceed the performance of methods that rely on both sparsity and quantization. Notably, quantization is orthogonal to our sparsity approach and could be combined with BSFA for additional speedups.¹

Metrics. We measure two primary metrics: **Time-to-first-token (TTFT)**: Wall-clock time for the prefill phase, averaged over 10 runs after warmup. **Task accuracy**: Task-specific metrics as defined by each benchmark, evaluated using the lm-evaluation-harness framework (Gao et al., 2024). Additionally, we validate threshold effectiveness by comparing **predicted density** and **measured density**. Predicted density represents the ideal fraction of causally reachable blocks we target: $\min(k, A)$ off-diagonal plus diagonal blocks, where A is the number of available non-diagonal blocks for a given query position. Measured density is the actual fraction retained when applying thresholds to validation data. To ensure rigorous evaluation, we measure both accuracy and latency on the *same* sequence lengths and samples for each sparsity configuration. This provides a direct comparison of the accuracy-speedup trade-off, as both metrics reflect performance on identical inputs rather than extrapolating from different sequence lengths.

5.2. Main Results

Table 1 and Figure 1 present our main results on the RULER benchmark. When maintaining at least 99% of baseline accuracy, BSFA achieves speedups of $1.03\times$ at 32K, $1.05\times$ at 64K, and $1.06\times$ at 128K. Most impressively, on the real-world LongBench benchmark (Table 2), BSFA achieves $1.10\times$ speedup while maintaining 99.1% of baseline accuracy with thresholds calibrated on the RULER dataset, demonstrating strong performance on practical tasks. At 32K with $k=192$, we observe a 0.5% accuracy improvement

¹We use the publicly available SpageAttention implementation exactly as provided in their Github repo for A100 GPUs, which includes their sparsity mechanism as well as INT8 quantization for Q/K blocks as part of their optimization strategy. We reached out to the authors to verify our results but received no response.

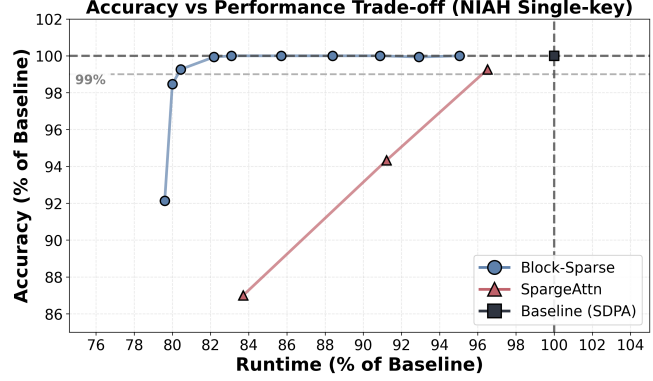


Figure 2. Performance on 64K Needle-in-a-Haystack task. BSFA maintains 99% accuracy even at extreme sparsity ($k=32$ blocks) while achieving $1.24\times$ speedup, demonstrating its ability to dynamically adapt to task requirements. Tasks requiring targeted retrieval can leverage aggressive sparsity without sacrificing accuracy.

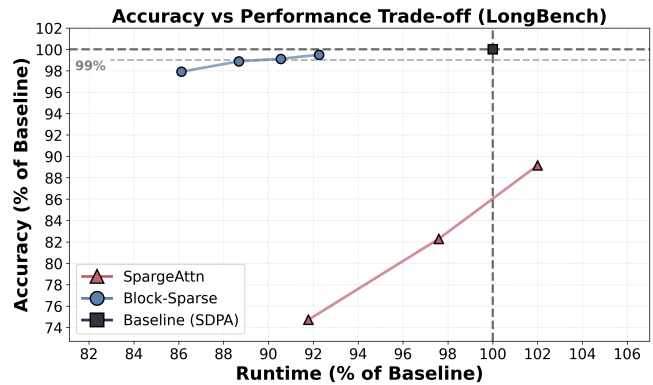


Figure 3. Accuracy vs. Time-to-First-Token (TTFT) speedup on LongBench benchmark. BSFA achieves consistent speedups while maintaining high accuracy, demonstrating effective cross-dataset generalization with thresholds calibrated on RULER.

over dense attention while matching its runtime, suggesting that selective attention based on exact scores can help models focus on the most relevant content. For applications that can tolerate modest accuracy trade-offs, speedups increase to $1.16\times$ at 128K with 96% accuracy retention. For targeted retrieval tasks like Needle-in-a-Haystack (Figure 2), BSFA achieves $1.24\times$ speedup at 64K while maintaining 99% accuracy, showcasing its task-adaptive nature.

Baseline comparisons demonstrate the advantages of exact score computation for sparsity decisions. SpageAttention, despite employing INT8 quantization for Q/K blocks, struggles to achieve practical speedups with acceptable accuracy. At 32K sequences, all SpageAttention configura-

Table 1. Main results on RULER benchmark across multiple sparsity levels (visualized in Figure 1). BSFA consistently outperforms other methods, maintaining near-baseline accuracy with reliable speedups. Speedup is computed as baseline time / method time, measured on the same tasks and sequence lengths as the accuracy results. Accuracy column shows absolute accuracy with degradation from baseline in brackets. Pred./Meas. Density shows calibrated density ratio vs measured density during inference (predicted/measured \pm std).

Seq Length	Method	Sparsity	Accuracy \uparrow	Pred./Meas. Density	Speedup \uparrow
32K	BSFA	Dense FlashAttention-2	All	85.98%	1.00
			$k=64$	84.94% (-1.2%)	0.24/0.28 \pm 0.04
			$k=96$	85.52% (-0.5%)	0.35/0.38 \pm 0.05
			$k=128$	86.00% (+0.0%)	0.45/0.47 \pm 0.05
			$k=192$	86.42% (+0.5%)	0.62/0.62 \pm 0.05
	SpargeAttention		$\tau=0.6$	75.62% (-12.1%)	-
			$\tau=0.75$	85.83% (-0.2%)	-
			$\tau=0.85$	86.18% (+0.2%)	-
64K	BSFA	Dense FlashAttention-2	All	84.96%	1.00
			$k=192$	83.08% (-2.2%)	0.35/0.36 \pm 0.05
			$k=256$	83.39% (-1.8%)	0.44/0.45 \pm 0.05
			$k=384$	84.24% (-0.8%)	0.62/0.61 \pm 0.05
	SpargeAttention		$\tau=0.3$	66.04% (-22.3%)	-
			$\tau=0.4$	75.07% (-11.6%)	-
			$\tau=0.5$	83.03% (-2.3%)	-
128K	BSFA	Dense FlashAttention-2	All	76.79%	1.00
			$k=512$	73.71% (-4.0%)	0.44/0.44 \pm 0.06
			$k=768$	75.75% (-1.4%)	0.61/0.61 \pm 0.05
			$k=1024$	76.54% (-0.3%)	0.76/0.74 \pm 0.05
	SpargeAttention		$\tau=0.5$	70.68% (-8.0%)	-
			$\tau=0.6$	75.28% (-2.0%)	-
			$\tau=0.7$	75.42% (-1.8%)	-

tions run slower than the dense baseline ($0.87\text{-}0.91\times$), with aggressive settings like $\tau=0.6$ sacrificing 12.1% accuracy while still running 9% slower. This likely occurs because of SpargeAttention’s overhead from its two-stage filtering pipeline, which first computes approximate scores on compressed tokens to generate a mask and then applies local filtering, outweighs the benefits from sparsity at these sequence lengths. In contrast, BSFA has minimal overhead since we make gating decisions inline during the existing FlashAttention computation, allowing us to achieve performance improvements even at these “shorter” sequence lengths (though 32K is substantial in absolute terms). This difference is most pronounced at moderate sequence lengths: while SpargeAttention requires longer sequences to amortize its mask computation overhead, BSFA provides consistent speedups across all evaluated lengths. At longer sequences, SpargeAttention’s performance improves but still cannot match our accuracy-speedup trade-offs. It either trades massive accuracy loss for modest speedups ($\tau=0.3$ with 22.3% accuracy loss for $1.19\times$ speedup) or achieves minimal speedup with notable degradation ($\tau=0.5$ with 2.3%

accuracy loss for only $1.03\times$ speedup). The sliding window baseline demonstrates the limitations of fixed patterns, achieving only 20.29% accuracy with 96 blocks, while BSFA with the same 96-block budget maintains 39.88% accuracy (nearly $2\times$ better). This stark contrast confirms that content-aware selection is essential for long-context understanding.

5.2.1. TASK-ADAPTIVE SPARSITY: NEEDLE-IN-A-HAYSTACK ANALYSIS

BSFA’s content-aware sparsity particularly excels at tasks requiring targeted information retrieval. Figure 2 presents results on the 64K Needle-in-a-Haystack Single-key task, where BSFA maintains 99% of baseline accuracy even at extreme sparsity, with only $k=32$ blocks, while achieving $1.24\times$ speedup. This contrasts sharply with the averaged RULER results in Table 1, where similar accuracy requires retaining 384 blocks. The disparity reveals BSFA’s task-adaptive nature. For needle-finding tasks where critical information concentrates in a few specific locations, our exact

Table 2. Accuracy on LongBench benchmark using thresholds calibrated on RULER dataset, demonstrating strong cross-dataset generalization (visualized in Figure 3). BSFA maintains high accuracy with speedups, while SpargeAttention shows accuracy-speed trade-offs and sliding window patterns perform poorly even with large window sizes. Speedup computed as baseline time / method time.

Method	Sparsity	Accuracy \uparrow	Speedup \uparrow
Dense FlashAttention-2	All	40.24%	1.00 \times
BSFA	$k=32$	39.39% (-2.1%)	1.16 \times
	$k=64$	39.78% (-1.1%)	1.13 \times
	$k=96$	39.88% (-0.9%)	1.10 \times
	$k=128$	40.03% (-0.5%)	1.08 \times
SpargeAttention	$\tau=0.4$	30.06% (-25.3%)	1.09 \times
	$\tau=0.5$	33.11% (-17.7%)	1.02 \times
	$\tau=0.6$	35.87% (-10.9%)	0.98 \times
Sliding Window	64 (4096 tokens)	13.43% (-66.6%)	-
	96 (6144 tokens)	20.29% (-49.6%)	-

score computation reliably identifies the few blocks containing relevant query-key interactions. The remaining blocks, containing only haystack distractors, receive uniformly low scores and can be safely skipped. This precision is particularly important for retrieval tasks. SpargeAttention’s approach of predicting block importance from compressed representations can miss critical information when the relevant content comprises only a small portion of a block. In contrast, our exact score computation examines every query-key interaction, ensuring we never miss high-scoring pairs regardless of their distribution within blocks. Tasks requiring broader contextual understanding (summarization, multi-hop reasoning) necessitate processing more blocks to capture distributed information. This suggests dynamic configurations are possible based on application requirements, with aggressive sparsity for document search, moderate for question answering, and minimal for holistic understanding tasks.

5.2.2. ROBUSTNESS AND GENERALIZATION

BSFA demonstrates strong robustness across diverse evaluation settings. The calibration process requires only 16 samples to produce thresholds that generalize effectively. As shown in the Pred./Meas. Density columns of Table 1, measured densities closely track predicted densities with low variance (see Metrics in 5.1 for detailed definitions). At 64K, we observe $36 \pm 5\%$ measured vs. 35% predicted for $k=192$ and $45 \pm 5\%$ vs. 44% for $k=256$. At 128K, the alignment is even stronger: $44 \pm 6\%$ measured vs. 44% predicted for $k=512$ and $61 \pm 5\%$ vs. 61% for $k=768$. This stability confirms that our thresholds capture consistent attention patterns across diverse inputs.

Cross-dataset generalization further validates our approach. Table 2 shows results on LongBench using thresholds calibrated exclusively on RULER samples. Despite LongBench

having fundamentally different task types and data distributions, including 12% Chinese language content, BSFA maintains 99.1% of baseline accuracy at $k=96$ with $1.10\times$ speedup. This represents our target operating point for general reasoning tasks, where we prioritize accuracy preservation. The method also supports more aggressive configurations ($k=32$) that achieve $1.16\times$ speedup with 97.9% accuracy retention for applications with different requirements. This generalization across languages and domains, using thresholds from an entirely different benchmark, demonstrates the robustness needed for practical deployment.

6. Conclusion

We presented Block-Sparse FlashAttention, a training-free method that accelerates long-context inference by computing exact query-key scores before selectively processing value blocks. Our key insight, that exact scores enable more reliable pruning decisions than approximation-based predictions, leads to a practical approach achieving $1.10\times$ speedup for general reasoning tasks and $1.24\times$ speedup for information retrieval, all while maintaining at least 99% of baseline accuracy. The method demonstrates strong robustness, with calibration on just 16 samples generalizing across datasets, languages, and task types. Unlike competing methods that sacrifice substantial accuracy or even run slower than baselines, BSFA provides consistent speedups with minimal accuracy impact. By achieving competitive performance using only selective computation in FP16, without requiring quantization, BSFA establishes that careful sparsity guided by exact scores is sufficient for practical acceleration, while remaining compatible with orthogonal optimizations for future improvements.

References

Bai, Y., Lv, X., Zhang, J., Lyu, H., Tang, J., Huang, Z., Du, Z., Liu, X., Zeng, A., Hou, L., Dong, Y., Tang, J., and Li, J. Longbench: A bilingual, multitask benchmark for long context understanding, 2024. URL <https://arxiv.org/abs/2308.14508>.

Beltagy, I., Peters, M. E., and Cohan, A. Longformer: The long-document transformer, 2020. URL <https://arxiv.org/abs/2004.05150>.

Child, R., Gray, S., Radford, A., and Sutskever, I. Generating long sequences with sparse transformers, 2019. URL <https://arxiv.org/abs/1904.10509>.

Choromanski, K., Likhoshesterov, V., Dohan, D., Song, X., Gane, A., Sarlos, T., Hawkins, P., Davis, J., Mohiuddin, A., Kaiser, L., Belanger, D., Colwell, L., and Weller, A. Rethinking attention with performers, 2022. URL <https://arxiv.org/abs/2009.14794>.

Dao, T. Flashattention-2: Faster attention with better parallelism and work partitioning, 2023. URL <https://arxiv.org/abs/2307.08691>.

Dao, T., Fu, D. Y., Ermon, S., Rudra, A., and Ré, C. Flashattention: Fast and memory-efficient exact attention with io-awareness, 2022. URL <https://arxiv.org/abs/2205.14135>.

Dong, Y., Cordonnier, J.-B., and Loukas, A. Attention is not all you need: Pure attention loses rank doubly exponentially with depth, 2023. URL <https://arxiv.org/abs/2103.03404>.

et al, A. G. The llama 3 herd of models, 2024. URL <https://arxiv.org/abs/2407.21783>.

et al, H. T. Llama: Open and efficient foundation language models, 2023a. URL <https://arxiv.org/abs/2302.13971>.

et al, J. A. Gpt-4 technical report, 2023b. URL <https://arxiv.org/abs/2303.08774>.

et al, S. B. Improving language models by retrieving from trillions of tokens, 2022. URL <https://arxiv.org/abs/2112.04426>.

et al, T. B. B. Language models are few-shot learners, 2020. URL <https://arxiv.org/abs/2005.14165>.

Gao, L., Tow, J., Abbasi, B., Biderman, S., Black, S., DiPofi, A., Foster, C., Golding, L., Hsu, J., Le Noac'h, A., Li, H., McDonell, K., Muennighoff, N., Ociepa, C., Phang, J., Reynolds, L., Schoelkopf, H., Skowron, A., Sutawika, L., Tang, E., Thite, A., Wang, B., Wang, K., and Zou, A. The language model evaluation harness, 07 2024. URL <https://zenodo.org/records/12608602>.

Gupta, A., Dar, G., Goodman, S., Ciprut, D., and Berant, J. Memory-efficient transformers via top- k attention, 2021. URL <https://arxiv.org/abs/2106.06899>.

Hsieh, C.-P., Sun, S., Kriman, S., Acharya, S., Rekesh, D., Jia, F., Zhang, Y., and Ginsburg, B. Ruler: What's the real context size of your long-context language models?, 2024. URL <https://arxiv.org/abs/2404.06654>.

Kitaev, N., Łukasz Kaiser, and Levskaya, A. Reformer: The efficient transformer, 2020. URL <https://arxiv.org/abs/2001.04451>.

Kojima, T., Gu, S. S., Reid, M., Matsuo, Y., and Iwasawa, Y. Large language models are zero-shot reasoners, 2022. URL <https://arxiv.org/abs/2205.11916>.

Lewis, P., Perez, E., Piktus, A., Petroni, F., Karpukhin, V., Goyal, N., Küttler, H., Lewis, M., tau Yih, W., Rocktäschel, T., Riedel, S., and Kiela, D. Retrieval-augmented generation for knowledge-intensive nlp tasks, 2020. URL <https://arxiv.org/abs/2005.11401>.

Lou, C., Jia, Z., Zheng, Z., and Tu, K. Sparser is faster and less is more: Efficient sparse attention for long-range transformers, 2024. URL <https://arxiv.org/abs/2406.16747>.

OpenAI. Gpt-4 technical report, 2024. URL <https://arxiv.org/abs/2303.08774>.

Roy, A., Saffar, M., Vaswani, A., and Grangier, D. Efficient content-based sparse attention with routing transformers, 2020. URL <https://arxiv.org/abs/2003.05997>.

Saada, T. N., Naderi, A., and Tanner, J. Mind the gap: a spectral analysis of rank collapse and signal propagation in attention layers. In *Forty-second International Conference on Machine Learning*, 2025. URL <https://openreview.net/forum?id=sRKtbGsebH>.

Tang, J., Zhao, Y., Zhu, K., Xiao, G., Kasikci, B., and Han, S. Quest: Query-aware sparsity for efficient long-context llm inference, 2024. URL <https://arxiv.org/abs/2406.10774>.

Vaswani, A., Shazeer, N., Parmar, N., Uszkoreit, J., Jones, L., Gomez, A. N., Kaiser, L., and Polosukhin, I. Attention is all you need, 2023. URL <https://arxiv.org/abs/1706.03762>.

Wei, J., Wang, X., Schuurmans, D., Bosma, M., Ichter, B., Xia, F., Chi, E. H., Le, Q. V., and Zhou, D. Chain-of-thought prompting elicits reasoning in large language models, 2022. URL <https://arxiv.org/abs/2201.11903>.

Xiao, G., Tian, Y., Chen, B., Han, S., and Lewis, M. Efficient streaming language models with attention sinks, 2024. URL <https://arxiv.org/abs/2309.17453>.

Xiong, Y., Zeng, Z., Chakraborty, R., Tan, M., Fung, G., Li, Y., and Singh, V. Nyströmformer: A nyström-based algorithm for approximating self-attention, 2021. URL <https://arxiv.org/abs/2102.03902>.

Zhang, J., Wei, J., Huang, H., Zhang, P., Zhu, J., and Chen, J. Sageattention: Accurate 8-bit attention for plug-and-play inference acceleration, 2025a. URL <https://arxiv.org/abs/2410.02367>.

Zhang, J., Xiang, C., Huang, H., Wei, J., Xi, H., Zhu, J., and Chen, J. Spargeattention: Accurate and training-free sparse attention accelerating any model inference, 2025b. URL <https://arxiv.org/abs/2502.18137>.

Zhang, Z., Sheng, Y., Zhou, T., Chen, T., Zheng, L., Cai, R., Song, Z., Tian, Y., Ré, C., Barrett, C., Wang, Z., and Chen, B. H₂O: Heavy-hitter oracle for efficient generative inference of large language models, 2023. URL <https://arxiv.org/abs/2306.14048>.

Zucchet, N., d’Angelo, F., Lampinen, A. K., and Chan, S. C. Y. The emergence of sparse attention: impact of data distribution and benefits of repetition, 2025. URL <https://arxiv.org/abs/2505.17863>.